ELSEVIER

Contents lists available at ScienceDirect

Composites Part B

journal homepage: www.elsevier.com/locate/compositesb



Extreme enhancement of the nonlinear elastic response of elastomer nanoparticulate composites via interphases



Amira B. Meddeb^a, Tim Tighe^b, Zoubeida Ounaies^a, Oscar Lopez-Pamies^{c,*}

- ^a Department of Mechanical and Nuclear Engineering, The Pennsylvania State University, State College, PA, 16802, USA
- ^b Materials Research Institute, The Pennsylvania State University, State College, PA, 16802, USA
- ^c Department of Civil and Environmental Engineering, University of Illinois, Urbana-Champaign, IL, 61801-2352, USA

ARTICLE INFO

Keywords: Nanocomposites Polymer confinement Rubber Finite strain

ABSTRACT

Over the last two decades, it has become increasingly unarguable that the addition of a small amount of nanoparticles to elastomers can lead to a drastic enhancement of their elastic response not only at small deformations but, more importantly, at large deformations. Yet, because of the experimental difficulties of conducting direct quantitative measurements of mechanical properties at the length scale of the nanoparticles together with the mathematical challenges associated with the analysis of large deformations in the presence of nanoscale heterogeneities, the precise mechanisms responsible for such an enhancement have remained unresolved. This paper reports a combined experimental/theoretical investigation aimed at revealing and quantifying the precise mechanisms behind the enhanced elastic properties of a prototypical class of elastomer nanoparticulate composites: polydimethylsiloxane (PDMS) filled with an isotropic distribution of TiO₂ nanoparticles. The synthesized composites exhibit drastically enhanced stress-stretch responses, featuring up to about a 10-fold increase with respect to the response of the unfilled PDMS elastomer, over the entire spectrum of small and large deformations considered. *Inter alia*, it is found that the "bulk" PDMS elastomer — i.e., the regions of the PDMS elastomer not immediately surrounding the nanoparticle aggregates formed during the synthesis process — is softer than the unfilled PDMS elastomer, while the "interphasial" PDMS elastomer surrounding the aggregates is significantly stiffer. The latter mechanism is found to rule over the former and to constitute the dominant mechanism behind the drastic enhancements in the macroscopic elastic properties of the composites.

1. Introduction and problem setting

Ever since the discovery [1,2] in the early 1900s that the addition of carbon black as reinforcing fillers could significantly improve the mechanical properties¹ of natural rubber, numerous investigators in a plurality of fields have studied the effects of adding nanoparticulate reinforcements to natural and synthetic elastomers. Owing to recent technical advances in the synthesis and characterization of soft organic solids embedding nanofillers, these studies have been increasingly intensified over the last two decades, see, e.g., [3–15]. In spite of the new insight furnished by all these recent efforts, the precise mechanisms responsible for the drastic macroscopic enhancement possibly afforded by the addition of nanofillers remain unresolved to date. This is because, at the experimental level, it remains difficult to carry out direct quantitative measurements of the local mechanical properties at the length scale of the nanoparticles and, at the theoretical level, until just

recently, the *mathematical difficulties* associated with the analysis of large deformations in the presence of nanoscale heterogeneities have hindered the necessary progress.

The purpose of this paper is to present a combined experimental/theoretical study aimed at revealing and quantifying the precise mechanisms behind the drastic enhancement of the *elastic response* of a prototypical synthetic elastomer — namely, a polydimethylsiloxane (PDMS) elastomer — by the addition of prototypical nanofillers — namely, equiaxed TiO₂ particles of about 10 nm in diameter — over small and large quasistatic deformations. The focus is on the fundamental case of uniform and isotropic additions of small amounts of nanofillers, specifically, less than 5% in volume fraction.

From an experimental point of view, the key ingredient in this study is the combined use of transmission electron microscopy (TEM) imaging to discern the make up of the nanoparticle aggregates resulting from the synthesis process at their respective length scale (in the order of tens of

^{*} Corresponding author.

E-mail address: pamies@illinois.edu (O. Lopez-Pamies).

¹ These include the linear and nonlinear elastic properties of rubber, as well as other of its mechanical properties, such as its fracture and abrasion.

A.B. Meddeb et al. Composites Part B 156 (2019) 166–173

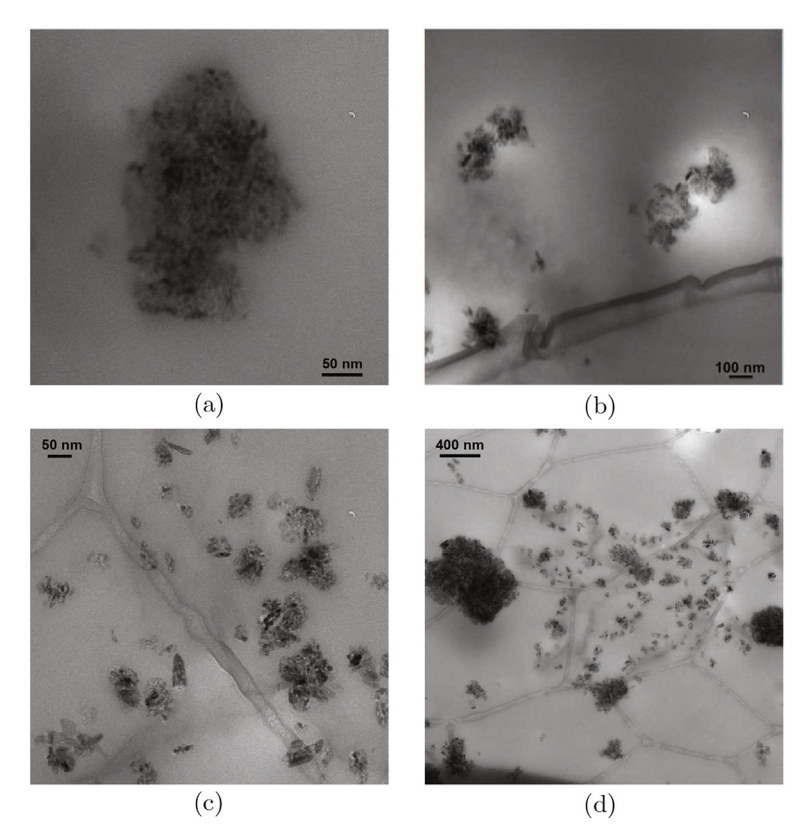


Fig. 1. Representative TEM images of two PDMS nanoparticulate composites. Parts (a) and (b) show two different resolutions of the same composite with 1% volume fraction of TiO₂ nanoparticles, while parts (c) and (d) show two different resolutions of another composite with the higher content of 4% volume fraction of TiO₂ nanoparticles. In these images, the darker and lighter regions correspond to the TiO₂ nanoparticles and the PDMS, respectively.

nanometers), of scanning electron microscopy (SEM) imaging to determine the size and shape dispersion of such aggregates, as well as the spatial distribution of these, at the larger length scale of microns, and of atomic force microscopy (AFM) measurements to estimate the thickness and the relative stiffness of the "interphasial" PDMS surrounding the aggregates compared to that of the "bulk" PDMS away from them. From the theoretical point of view, the key ingredient is the use of a recent homogenization result [16] that describes the macroscopic elastic response of a given isotropically filled elastomer at arbitrarily large deformations directly in terms of: (i) the elastic properties of the "bulk" elastomer away from the fillers, (ii) the thickness and elastic properties of the "interphasial" elastomer surrounding the fillers, (iii) the content of fillers, and (iv) the content of "occluded" elastomer trapped in filler agglomerates or aggregates.

We begin in Section 2 by describing the synthesis and characterization of the class of PDMS nanoparticulate composites studied in this work. That section includes representative TEM and SEM images of the underlying nanostructures of composites featuring various contents of TiO₂ nanoparticles. Section 3 provides representative results from AFM measurements of the local stiffness of the PDMS elastomer within the nanoparticulate composites. In Section 4, we present the macroscopic uniaxial stress-stretch response of several specimens that show that the addition of small amounts (less than 5% in volume fraction) of TiO₂ nanoparticles can stiffen the elastic response of PDMS, at small as well as at large deformations, *up to about one order of magnitude*. With help of the aforementioned homogenization result, this extreme enhancement of macroscopic properties is explained directly in terms of the TEM and SEM imaging as well as of the AFM stiffness measurements in Section 5. There we also record the main conclusions of this work.

2. Synthesis and characterization of the PDMS nano-particulate composites

2.1. Synthesis

In this work, the elastomer used in all the synthesized nanoparticulate composites is Sylgard 184, a popular PDMS elastomer from Dow Corning [17,18], and the nanofillers are equiaxed anatase ${\rm TiO_2}$ particles, acquired from NanoAmor, of roughly 10 nm in diameter. In all the specimens, the solvent n-heptane was used to reduce the viscosity of the PDMS and poly (ethylene glycol) was used as a surfactant, both of which were purchased from Sigma Aldrich.

The synthesis of all the specimens started with thoroughly mixing in a 9:1 weight ratio the PDMS base and the n-heptane solvent. As a second step, the surfactant was dissolved in the PDMS solution, then, the desired amount of nanoparticles was added; the surfactant to nanoparticles ratio was 1:5 by weight. Immediately after its preparation, the solution containing the nanoparticles was magnetically stirred for 8 h. Following the stirring, the curing agent was added to the solution in a ratio of PDMS base to curing agent of 9:1 by weight, then the solution was further stirred for about 5 min and subsequently degassed to remove any air bubbles. Once all the optically visible bubbles were removed, the solution was cast on a glass plate covered with a very thin layer of a release agent. This was then cured at 120 °C for about 1 h for the pure PDMS and for about 6 h for the composites; these curing temperature and times were selected so as to ensure completion of the cross-linking process, c. f., [18]. The thickness of the resulting film was uniform, but varied between 200 and 300 μm for different films. Three different specimens were cut out from each synthesized film for mechanical testing, while the remainder of the film was used for the characterization of the underlying nanostructure.

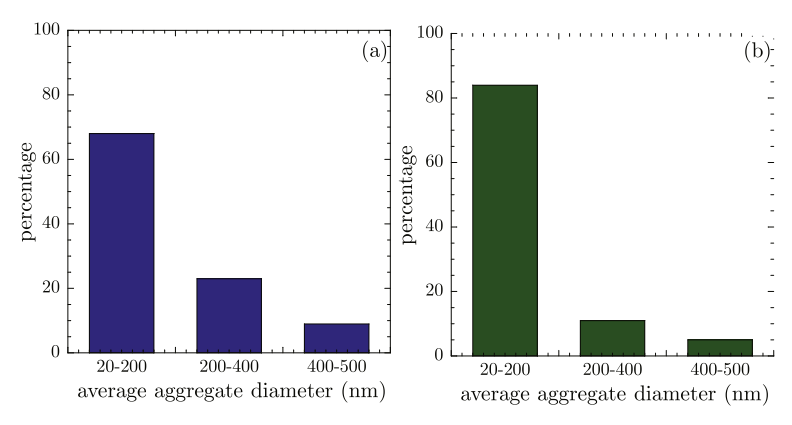


Fig. 2. Distribution of the average diameter of aggregates in the same two PDMS nanoparticulate composites shown in Fig. 1, generated from a plurality of TEM images of the samples. Part (a) corresponds to the composite with 1% volume fraction of TiO₂ nanoparticles, while part (b) corresponds to the composite with 4%.

2.2. Microscopy characterization

Once a film was fabricated, we proceeded with the characterization of its nanostructure at the scales of tens of nanometers via TEM and of microns via SEM; in particular, we made use of a Philips 420 TEM and a FESEM Nova Nano 630.

Fig. 1 (a)-(b) show representative TEM images, at two different resolutions, of a composite with 1% volume fraction of TiO2 nanoparticles. One salient observation from these images is that the nanoparticles do not appear as single inclusions embedded within the PDMS elastomer, but rather, as aggregates. These are equiaxed in shape and polydisperse in size ranging from 20 to 500 nm in average diameter (recall that the TiO₂ nanoparticles used in the synthesis are roughly 10 nm in diameter), with about 75% of these ranging only from 20 nm to 200 nm; see Fig. 2. Another key observation is that the aggregates are comprised of a collection of single TiO2 nanoparticles bonded together through thin layers of the PDMS elastomer. What is more, irrespectively of the size of the aggregate, the content in volume of such thin layers per aggregate is about the same as that of TiO2 nanoparticles. This can be seen from the representative aggregate shown in Fig. 1(a), wherein the darker regions correspond to the TiO2 nanoparticles, whereas the lighter regions correspond to the PDMS.

Fig. 1(c)–(d) show TEM images analogous to those shown in Fig. 1(a)–(b), but for a composite with the higher content of 4% volume fraction of ${\rm TiO_2}$ nanoparticles. These images illustrate that the same features outlined above for the composite with 1% volume fraction of ${\rm TiO_2}$ nanoparticles apply to composites with different content of ${\rm TiO_2}$ nanoparticles, namely, that: (i) the nanoparticles appear in the form of equiaxed aggregates ranging from 20 to 500 nm in average diameter, but with most of these ranging only from 20 to 200 nm, (ii) the aggregates are comprised of ${\rm TiO_2}$ nanoparticles bonded together through thin layers of PDMS elastomer, and (iii) the content in volume of ${\rm TiO_2}$ nanoparticles and PDMS elastomer per aggregate is roughly the same. These three features held true for all the composites that we studied, which contained a volume fraction of ${\rm TiO_2}$ nanoparticles that ranged from 0.05% to 4%.

Fig. 3 presents SEM images of the same two composites shown in Fig. 1 at the larger length scale of microns. These images provide further evidence that the aggregates of ${\rm TiO_2}$ nanoparticles are equiaxed in shape and polydisperse in size, irrespectively of the volume fraction of nanoparticles. They also confirm that the aggregates are uniformly and isotropically distributed in space throughout the specimen.

3. The local elastic response of the PDMS elastomer within the nanoparticulate composites

In the context of elastomer nanoparticulate composites, it is by now well established [9,19–27] that the presence of nanofillers has two

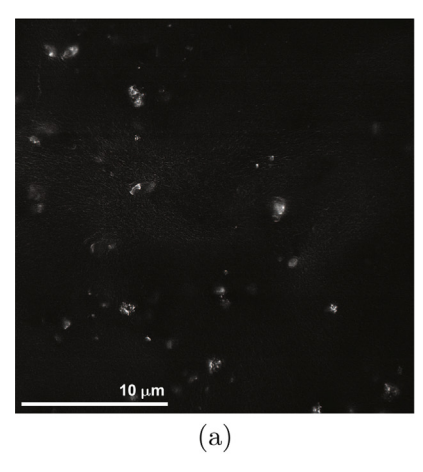
major effects on the embedding elastomer: (i) the "interphasial" elastomer surrounding the nanofillers — often referred to in the literature as "bound rubber" — exhibits a significantly *stiffer* response than the "bulk" elastomer away from them, and (ii) the "bulk" elastomer away from the nanofillers exhibits a *different* — typically *softer*— mechanical response from that of the same elastomer synthesized in the absence of nanofillers. The stiffer response of the "interphasial" elastomer stems from the different conformations that the polymer chains have to adopt to attach to the nanofillers. The different response of the "bulk" elastomer away from the nanofillers is mostly due to the fact that their presence disrupts the cross linking process. In spite of this well established *qualitative* insight, there is little *quantitative* understanding of how much of the elastomer is "interphasial" or "bulk" and of what their elastic properties are, especially their nonlinear elastic properties at large deformations.

As anticipated in the Introduction, in this work we make use of AFM to estimate the content and the linear elastic properties of the "interphasial" PDMS elastomer relative to that of the "bulk" PDMS elastomer in the nanoparticulate composites under investigation.² In particular, we carried out AFM measurements using a Bruker Dimension Icon in PeakForce Tapping mode. A Scanasyst-Air probe was used featuring a SiN cantilever beam with 0.4 N/m spring constant and a Si tip with 2 nm nominal radius of curvature. A relative calibration³ was done using PDMS-Soft-1-12 M Bruker PFQNM standard with a nominal Young's modulus of 2.5 MPa. Assuming that the PDMS elastomer within the composites is an incompressible elastic solid with locally isotropic properties, we made use of the Derjaguin-Muller-Toporov model [28] to transcribe the AFM measurements into a local shear modulus μ_{local} (recall that for an isotropic incompressible elastic solid the shear modulus μ is related to the Young's modulus E by $E = 3\mu$). We emphasize that the values of μ_{local} generated by this procedure are not expected to be accurate in an absolute sense, but, as elaborated in the remaining of this section, they provide precious semi-quantitative insight into the geometry of the domains occupied by the "interphasial" PDMS elastomer and the stiffness of this relative to the stiffness of the "bulk" PDMS elastomer.

Fig. 4(a) and (b) present AFM measurements of the local shear

 $^{^2}$ For all practical purposes, given that the shear modulus of TiO₂ is in the order of 100 GPa whereas that of PDMS is in the order of 1 MPa, the TiO₂ nanoparticles can be considered as mechanically rigid.

 $^{^3}$ In a relative calibration, the deflection sensitivity (Nm/V) of the probe is measured on a hard standard (typically sapphire), then, the PDMS standard is measured while the spring constant and radius of the probe are adjusted to report the standard modulus at the correct value at that particular deformation depth (typically 2–5 nm). Unknowns are measured by engaging the surface and adjusting the force set point to match the standards calibration deformation depth.



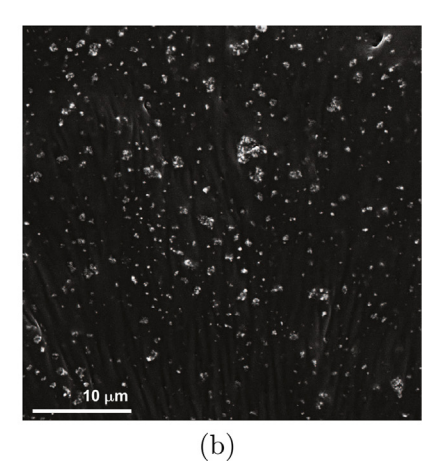


Fig. 3. SEM images of the same two PDMS nanoparticulate composites shown in Fig. 1. The image in part (a) corresponds to the composite with 1% volume fraction of TiO₂ nanoparticles, while that of part (b) corresponds to the composite with the higher content of 4%.

modulus μ_{local} of the unfilled PDMS elastomer. Specifically, the contour plot displayed in part (a) over a representative $1~\mu m \times 1~\mu m$ domain of the specimen surface shows that the local shear modulus exhibits pointwise values in the range [3.3, 5.9] MPa and an average value of about 5.4 MPa. These values, which are consistent with those reported in the literature for the same type of PDMS [29], are easier to visualize from the plot displayed in part (b) of the figure, which shows the variation of the shear modulus along the solid line traced on the contour plot in part (a).

Turning now to the nanoparticulate composites, Fig. 4(c) and (d) present AFM measurements of the local shear modulus μ_{local} of the PDMS elastomer around a typical particle aggregate within a composite with 0.5% volume fraction of TiO2 nanoparticles. Similar to Fig. 4(a) and (b), part (c) of the figure provides a contour plot of μ_{local} , while part (d) provides the value of μ_{local} along the solid line traced on the contour plot in part (c). There are three main observations from these results. First, according to the results along the solid line, the thickness of the "interphasial" PDMS elastomer surrounding the particle aggregate is in the order of half the diameter of the aggregate, in this case, about 160 nm. Here, it is important to note that the thickness of the "interphasial" PDMS elastomer surrounding smaller particle aggregates (than the one shown in Fig. 4(c)) are typically relatively larger, possibly as large as the diameter of the aggregate that they surround. Second, the same results also indicate that the shear modulus of the "interphasial" PDMS elastomer is not homogenous but increasingly stiffer closer to the aggregate, with shear modulus values ranging from 1 to about 8 times that of the "bulk" PDMS elastomer away from the aggregate. Third, the results along the solid line also reveal that the shear modulus of the "bulk" PDMS elastomer is essentially homogeneous and smaller than that of the unfilled PDMS elastomer. In particular, we note that the shear modulus of the "bulk" PDMS elastomer in the composite is, on average, about 3.0 MPa, while that of the unfilled PDMS elastomer is, again, on average, about 5.4 MPa.

Fig. 4(e)–(f) and (g)–(h) present AFM measurements entirely analogous to those put forth by Fig. 4(c)–(d), but for composites with the higher content of 1% and 4% volume fraction of TiO_2 nanoparticles. Qualitatively, the same three main observations recorded above for the composite with 0.5% volume fraction of TiO_2 nanoparticles apply to the composites with volume fractions 1% and 4%. Quantitatively, however, there is a major difference: the shear modulus of the "bulk" PDMS elastomer away from the aggregates decreases significantly with increasing content of TiO_2 nanoparticles. More specifically, the average shear modulus of the "bulk" PDMS elastomer in the composite with 1% of TiO_2 nanoparticles is about 2.31 MPa, while that of the "bulk" PDMS elastomer in the composite with 4% is about 0.48 MPa.

4. The macroscopic elastic response of the nanoparticulate composites

Having determined the geometric makeup of the synthesized PDMS nanoparticulate composites across the several relevant length scales, as well as the local stiffness of the underlying PDMS elastomer relative to that of the unfilled PDMS elastomer, we now turn to examining their macroscopic elastic response.

Given that the PDMS nanoparticulate composites were fabricated in the form of films (again, with thicknesses varying from 200 to 300 μm), we examined their macroscopic response via uniaxial tensile stress-stretch tests. These were performed in a RSA-G2 analyzer from TA Instruments at a constant stretch rate of $10^{-3}~s^{-1}$, which was checked to be sufficiently slow for dissipative effects to be negligible. For each value of volume fraction of nanoparticles that we considered, we fabricated two films. Further, as already mentioned above, we cut and tested three different specimens from each of the fabricated films. Up to the expected variations in the stretch at which they failed, 4 the difference in the stress-stretch response between any two specimens from the same or a different film with the same volume fraction of nanoparticles was less than 1%.

Fig. 5 shows the nominal uniaxial stress S in terms of the applied stretch λ for the unfilled PDMS elastomer (solid triangles) and for PDMS nanoparticulate composites (solid circles) with 0.5%, 1%, and 4% volume fraction of ${\rm TiO_2}$ nanoparticles; the (solid and dashed) lines stand for the corresponding theoretical results discussed in the next section. Table 1 records the shear modulus μ extracted from these macroscopic experiments for all four sets of data. We remark that the results for the specific values of 0.5%, 1%, and 4% reported here are representative of the results for the entire range of volume fractions from 0% to 5%.

The chief observation from Fig. 5 is that small additions (less than 5% in volume fraction) of TiO_2 nanoparticles lead to drastic enhancements of the elastic response of PDMS over the entire range of deformations. At small deformations, Table 1 indicates that the addition of a mere 0.5% of TiO_2 nanoparticles leads to a remarkable 2-fold increase of the shear modulus over that of the unfilled PDMS elastomer, while the addition of just 1% leads to an even more remarkable 4-fold increase. Interestingly, the addition of 4% of TiO_2 nanoparticles leads to a 3-fold increase, certainly still remarkable but, interestingly, a smaller increase than that afforded by 1%. At large deformations, the same qualitative trends hold. Quantitatively, the stress-stretch responses of the composites with 0.5%, 1%, and 4% of TiO_2 nanoparticles reach to be

⁴Failure of the specimens occurs from the macroscopic propagation of a crack that nucleates from a surface defect on their boundary and thus it is a stochastic process.

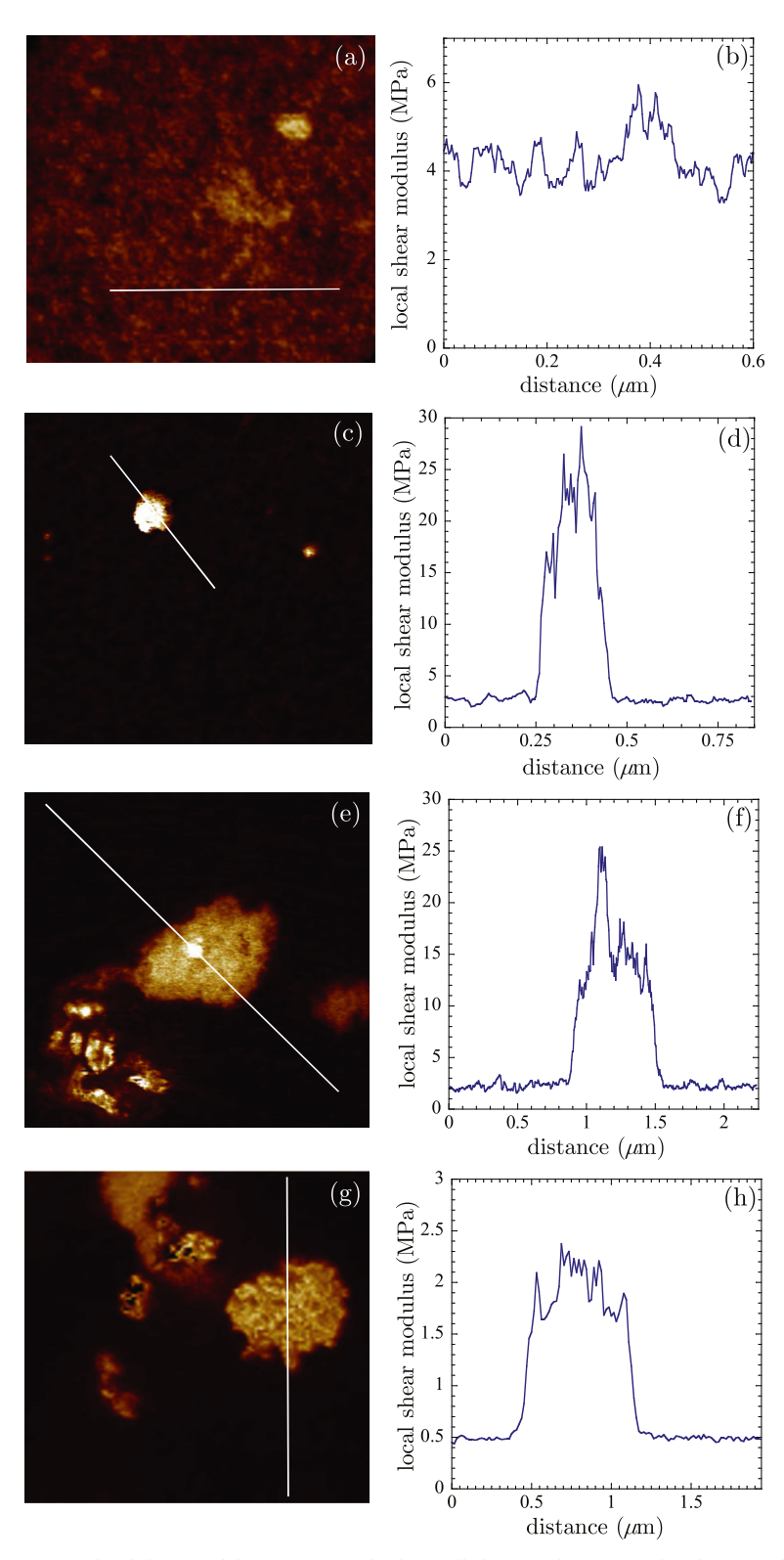


Fig. 4. Illustrative AFM measurements of the local shear modulus μ_{local} of (a)–(b) the unfilled PDMS elastomer and of the "interphasial" and "bulk" PDMS elastomer within nanoparticulate composites with (c)–(d) 0.5%, (e)–(f) 1%, and (g)–(h) 4% volume fractions of TiO₂ nanoparticles. Note that the length of each of the solid lines traced over the AFM images is given by the abscissae in the plots.

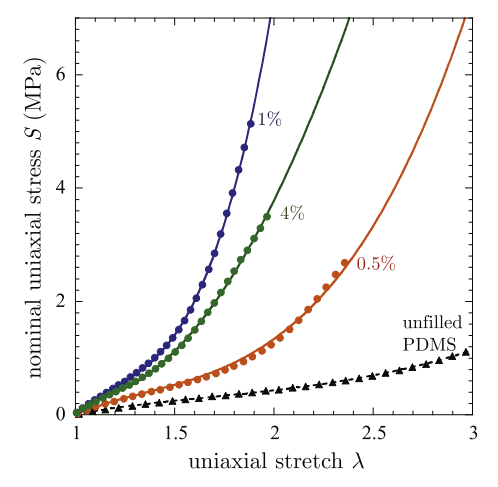


Fig. 5. Uniaxial stress-stretch response of the unfilled PDMS elastomer and of PDMS nanoparticulate composites with 0.5%, 1%, and 4% volume fraction of TiO_2 nanoparticles. The discrete symbols (solid triangles and circles) correspond to experimental measurements, while the (solid and dashed) lines stand for the corresponding theoretical results given by the homogenization formula (4) with the parameters listed in Tables 2 and 3.

Table 1 Shear modulus μ determined from the macroscopic stress-stretch experiments reported in Fig. 5 of the unfilled PDMS elastomer and the PDMS nanoparticulate composites.

Vol. % of TiO ₂ nanoparticles	0	0.5	1	4
Shear modulus μ (MPa)	0.24	0.49	1.02	0.75

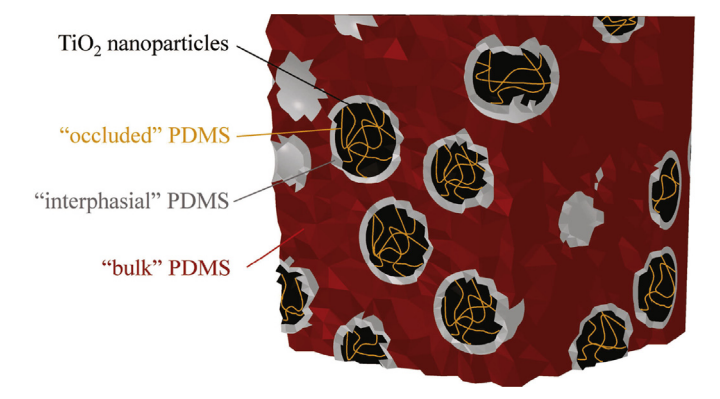


Fig. 6. Schematic description of the PDMS nanoparticulate composites at the length scale of the nanoparticle aggregates.

about 4, 12, and 8 times stiffer than the stress-stretch response of the unfilled PDMS elastomer.

5. Theoretical analysis and conclusions

In the sequel, we explain and describe the above extreme macroscopic elastic response of the PDMS nanoparticulate composites directly in terms of the microscopy results presented in Sections 2 and 3.

We begin by remarking that Sections 2 and 3 have provided a complete *qualitative* description of the PDMS nanoparticulate composites under investigation here, from the nanometer length scale of the ${\rm TiO_2}$ nanoparticles to the centimeter length scale of the fabricated films. In a nutshell, as schematically depicted by Fig. 6, the synthesized composites are comprised of a random and isotropic distribution of nanoparticle aggregates bonded to a homogenous "bulk" PDMS elastomer through a heterogeneous "interphasial" PDMS elastomer. The

aggregates are equiaxed in shape, polydisperse in size, and are comprised of a mixture of ${\rm TiO_2}$ nanoparticles and "occluded" PDMS elastomer firmly bonded together. The microscopy results have also provided some *semi-quantitative* insight: (i) the content in volume of "occluded" PDMS elastomer is roughly equal to the content of ${\rm TiO_2}$ nanoparticles, (ii) the thicknesses of the regions occupied by the "interphasial" PDMS elastomer range from half to the full diameter of the aggregates that they surround, (iii) the "interphasial" PDMS elastomer is significantly stiffer than the "bulk" PDMS elastomer, and (iv) the "bulk" PDMS elastomer is softer than the unfilled PDMS elastomer, increasingly so for composites with higher content of ${\rm TiO_2}$ nanoparticles.

Now, by leveraging current advances in iterative and comparison-medium nonlinear homogenization methods [30–32], Goudarzi et al. [16] have recently derived a homogenization result that describes the macroscopic elastic behavior of a fairly general class of filled elastomers directly in terms of their nanoscopic (or microscopic) behavior. When specialized to the class of PDMS nanoparticulate composites of interest here — as schematically described by Fig. 6 and wherein the "interphasial" PDMS elastomer is significantly stiffer than the "bulk" PDMS elastomer⁵ — the result states that their macroscopic elastic response is characterized by the stored-energy function

$$W(\mathbf{F}) = \begin{cases} (1 - c_p - c_o - c_i)\Phi_{bulk}(\mathscr{I}_1) & \text{if det } \mathbf{F} = 1\\ + \infty & \text{otherwise} \end{cases}$$
(1)

with

$$\mathscr{I}_1 = \frac{I_1 - 3}{(1 - c_n - c_0 - c_i)^{7/2}} + 3,$$

where c_p , c_o , c_i stand for, respectively, the volume fractions of nanoparticles, "occluded" PDMS elastomer, and "interphasial" PDMS elastomer, and where $\Phi_{bulk}(I_1)$ is the (bounded branch of the) stored-energy function that characterizes the elastic response of the "bulk" PDMS elastomer, with $I_1 = F_{ij}F_{ij}$ denoting the first principal invariant associated with the deformation gradient tensor **F**. For use in the analysis of the macroscopic experimental data presented in Section 4, we recall that the stress-stretch response implied by the stored-energy function (1) for uniaxial loading, when $I_1 = \lambda^2 + 2\lambda^{-1}$, is given by

$$S = \frac{2(\lambda - \lambda^{-2})}{(1 - c_p - c_o - c_i)^{5/2}} \Phi'_{bulk} \left(\frac{\lambda^2 + 2\lambda^{-1} - 3}{(1 - c_p - c_o - c_i)^{7/2}} + 3 \right), \tag{2}$$

where, again, S denotes the nominal uniaxial stress, λ is the applied stretch, and where we have made use of the standard convention $\Phi'_{bulk}(I_1) \doteq d\Phi_{bulk}(I_1)/dI_1$ to denote the derivative of $\Phi_{bulk}(I_1)$ with respect to its sole scalar argument.

In this work, we shall make use of the stored-energy function [33].

$$\Phi_{bulk}(I_1) = \sum_{r=1}^{2} \frac{3^{1-\alpha_r}}{2\alpha_r} \mu_r \left[I_1^{\alpha_r} - 3^{\alpha_r} \right]$$
(3)

for the "bulk" PDMS elastomer within the composites. In this expression, μ_r are real-valued material parameters whose addition amounts to the shear modulus of the elastomer (namely, $\mu_1 + \mu_2 = \mu_{bulk}$), while α_r are real-valued material parameters that describe the non-Gaussian stiffening of the elastomer at large deformations [33]. In addition to its mathematical simplicity and physical meaning of its parameters, we choose the class of stored-energy functions (3) to model the "bulk" PDMS because of its rich functional form and demonstrated descriptive

⁵ In particular, Goudarzi et al. [16] showed that when the "interphasial" elastomer is 5 or more times stiffer than the "bulk" elastomer, it can be approximated — irrespectively of its heterogeneity or anisotropy and for all practical purposes of computing the macroscopic elastic response of the composite — as mechanically rigid. This is because most of the deformation localizes in the 'bulk" elastomer in such cases.

Table 2 Volume fraction of the "occluded" and the "interphasial" PDMS elastomer within the composites with 0.5%, 1%, and 4% volume fraction of TiO_2 nanoparticles.

	c_o	c_i
0.5% vol. TiO ₂	0.005	0.2503
1% vol. TiO ₂	0.01	0.4552
4% vol. TiO ₂	0.04	0.5863

Table 3 Material parameters in the stored-energy function (3) used to describe the elastic response of the "bulk" PDMS elastomer within the composites with 0.5%, 1%, and 4% volume fraction of TiO_2 nanoparticles. The corresponding materials parameters that describe the elastic response of the unfilled PDMS elastomer are also included for comparison.

	μ_1 (MPa)	α_1	μ_2 (MPa)	α_2
Unfilled PDMS	0.1878	0.3250	0.0524	2.5164
0.5% vol. TiO_2	0.1802	0.3087	0.0519	2.5541
1% vol. TiO ₂	0.1673	0.3249	0.0361	2.5479
4% vol. ${\rm TiO_2}$	0.0553	0.3245	0.0102	1.7410

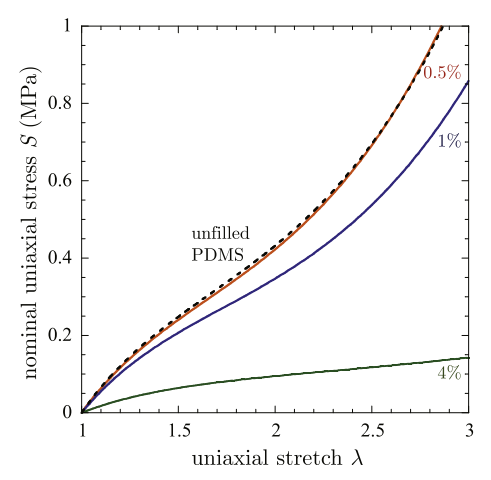


Fig. 7. Uniaxial stress-stretch response of the "bulk" PDMS elastomer within the composites with 0.5%, 1%, and 4% volume fraction of ${\rm TiO_2}$ nanoparticles. The response of the unfilled PDMS elastomer (dashed line) is also displayed for comparison.

and predictive capabilities [33,34]. The specialization of the macroscopic uniaxial stress-stretch relation (2) for the case when the elastic response of the "bulk" PDMS elastomer is characterized by (3) takes the simple explicit form

$$S = \frac{\lambda - \lambda^{-2}}{(1 - c_p - c_o - c_i)^{5/2}} \sum_{r=1}^{2} 3^{1 - \alpha_r} \mu_r \left(\frac{\lambda^2 + 2\lambda^{-1} - 3}{(1 - c_p - c_o - c_i)^{7/2}} + 3 \right)^{\alpha_r}.$$
 (4)

We are now in a position to make use of the formula (4) to analyze the macroscopic experimental data presented in Section 4. To this end, we emphasize that the volume fraction c_p of TiO_2 nanoparticles is a known quantity from the outset, and so is the volume fraction c_o of "occluded" PDMS elastomer, in particular, $c_o = c_p$. On the other hand, the value of the volume fraction c_i of "interphasial" PDMS elastomer and the elastic response of the "bulk" PDMS elastomer, as characterized by the material parameters μ_r and α_r in (4), are *not* known. We do have some partial information about them from the AFM measurements. Namely, we do know that the volume fraction c_i of "interphasial" PDMS elastomer should be in the range $8(c_p + c_o) = (1 + 2t_{min}/d)^3(c_p + c_o) \leq c_i \leq (1 + 2t_{max}/d)^3(c_p + c_o) = 27(c_p + c_o)$, since the minimum t_{min} and maximum t_{max} values of the thickness t of the

interphases are roughly given by half d/2 and the full diameter d of the aggregates that they surround. We also know that the "bulk" PDMS elastomer is softer than the unfilled PDMS elastomer, again, increasingly so for composites with higher content of TiO_2 nanoparticles. We proceed then by taking the parameters c_i , μ_1 , μ_2 , α_1 , α_2 as unknowns and by fitting (via least squares) the relation (4) to the stress-stretch experimental data presented in Fig. 5. The results for c_i , μ_1 , μ_2 , α_1 , α_2 from this fitting are presented in Tables 2 and 3 for the three PDMS nanoparticulate composites with 0.5%, 1%, and 4% volume fraction of TiO_2 nanoparticles. The resulting stress-stretch relations are included in Fig. 5 for direct comparison with the experimental data. The agreement between the theoretical and experimental stress-stretch results for all three composites is remarkably good over the entire range of deformations.

The values of the parameters c_i , μ_1 , μ_2 , α_1 , α_2 in Tables 2 and 3 obtained from the macroscopic response of the composites via the homogenization result (4) are in complete agreement with the semiquantitative AFM local measurements. Indeed, the values of the volume fraction c_i of "interphasial" PDMS elastomer correspond to interphase thicknesses that are between half and the full diameter of the particle aggregates that they surround. Moreover, the values of the material parameters $\mu_1, \mu_2, \alpha_1, \alpha_2$ characterizing the elastic response of the "bulk" PDMS elastomer within each of the three composites with 0.5%, 1%, and 4% volume fraction of TiO2 nanoparticles correspond to increasingly softer elastomers than the unfilled PDMS elastomer. This is easier to visualize from Fig. 7, where the uniaxial stress-stretch response of the "bulk" PDMS elastomer within each of the composites is compared to one another and to the response of the unfilled PDMS elastomer. We notice from these that the "bulk" PDMS elastomer within the composite with 4% volume fraction of TiO₂ nanoparticles is markedly softer than that within the composite with 1% volume fraction. This is why the corresponding macroscopic response of the composite is also softer, in spite of containing a larger content of reinforcing nanoparticles.

The above theoretical quantitative results, in conjunction with the experimental results presented in Sections 2 through 3, indicate that:

- the presence of stiff interphases is the dominant mechanism behind the drastically enhanced macroscopic elastic response of the PDMS nanoparticulate composites;
- the "interphasial" enhancement is so dominant that it overcomes the softening afforded by the presence of a "bulk" PDMS elastomer that, remarkably, can be significantly softer than the unfilled PDMS elastomer; and
- the presence of "occluded" PDMS elastomer constitutes also a stiffening mechanism, but its effect is only marginal.

Because of the prototypical nature of PDMS as an elastomer and of ${\rm TiO_2}$ nanoparticles as nanofillers, we expect that these conclusions remain largely applicable to other types of elastomer nanoparticulate composites with small amounts of nanofillers.

At the close of these conclusions, we remark that the quantitative results reported in this paper further reinforce the idea that judicious manipulation of interphasial phenomena in elastomer nanoparticulate composites — especially those with a dilute content of nanoparticles — provides a promising path forward for the design of materials with exceptional mechanical and other physical properties, see, e.g., [35–39].

Acknowledgements

Support for this work by the National Science Foundation, US through the collaborative Grants CMMI-1661853 and CMMI-1662720 is gratefully acknowledged.

Appendix A. Supplementary data

Supplementary data related to this article can be found at https://doi.org/10.1016/j.compositesb.2018.08.064.

References

- Wiegand WB. The carbon reinforcement of rubber. Rubb. Chem. Tech. 1937;10:395–411.
- [2] Leblanc JL. Filled polymers: science and idustrial applications. Boca Raton: CRC Press: 2010.
- [3] Berriot J, Montes H, Lequeux F, Long D, Sotta P. Evidence for the shift of the glass transition near the particles in silica-filled elastomers. Macromolecules 2002;35:9756–62.
- [4] Frogley D, Ravich D, Wagner HD. Mechanical properties of carbon nanoparticlereinforced elastomers. Compos Sci Technol 2003;63:1647–54.
- [5] Ramier J. Comportement mécanique d'élastomères chargés, influence de l'adhésion chargepolymère, influence de la morphologie [PhD Thesis] France: Institut National des Sciences Appliquées de Lyon; 2004.
- [6] Crosby AJ, Lee J-Y. Polymer nanocomposites: the "nano" effect on mechanical properties. Polym Rev 2007;47:217–29.
- [7] Zou H, Wu S, Shen J. Polymer/silica nanocomposites: preparation, characterization, properties, and applications. Chem Rev 2008;108:3893–957.
- [8] Yousefi M, Gholamian F, Ghanbari D, Masoud Salavati-Niasari M. Polymeric nanocomposite materials: preparation and characterization of star-shaped PbS nanocrystals and their influence on the thermal stability of acrylonitrile-butadiene-styrene (ABS) copolymer. Polyhedron 2011;30:1055–60.
- [9] Qu M, Deng F, Kalkhoran SM, Gouldstone A, Robisson A, Van Vliet KJ. Nanoscale visualization and multiscale mechanical implications of bound rubber interphases in rubber-carbon black nanocomposites. Soft Matter 2011;7:1066–77.
- [10] Qu L, Yu G, Wang L, Li C, Zhao Q, Li J. Effect of filler-elastomer interactions on the mechanical and nonlinear viscoelastic behaviors of chemically modified silica-reinforced solution-polymerized styrene butadiene rubber. J Appl Polym Sci 2012;126:116–26.
- [11] Liu H, Zhang L, Yang D, Yu Y, Yao L, Tian M. Mechanical, dielectric, and actuated strain of silicone elastomer filled with various types of TiO₂. Soft Mater 2012;11:363–70.
- [12] Ganesan V, Jayaraman A. Theory and simulation studies of effective interactions, phase behavior and morphology in polymer nanocomposites. Soft Matter 2014;10:13–38.
- [13] Tadiello L, D'Arienzo M, Di Credico B, Hanel T, Matejka L, Mauri M, Morazzoni F, Simonutti R, Spirkovac M, Scotti R. The filler-rubber interface in styrene butadiene nanocomposites with anisotropic silica particles: morphology and dynamic properties. Soft Matter 2015;11:4022–33.
- [14] Ghiyasiyan-Arani M, Masjedi-Arani M, Ghanbari D, Bagheri S, Salavati-Niasari M. Novel chemical synthesis and characterization of copper pyrovanadate nanoparticles and its influence on the flame retardancy of polymeric nanocomposites. Sci Rep 2015;6:25231.
- [15] Zhao L, Li J, Li Z, Zhang Y, Liao S, Yu R, Hui D. Morphology and thermomechanical properties of natural rubber vulcanizates containing octavinyl polyhedral oligomeric silsesquioxane. Composites Part B 2018;139:40–6.
- [16] Goudarzi T, Spring DW, Paulino GH, Lopez-Pamies O. Filled elastomers: A theory of filler reinforcement based on hydrodynamic and interphasial effects. J Mech Phys Solid 2015;80:37–67.
- [17] https://consumer.dow.com/content/dam/dcc/documents/en-us/ productdatasheet/11/11-31/11-3184-sylgard-184-elastomer.pdf?iframe=true.
- [18] Johnston ID, McCluskey DK, Tan CKL, Tracey MC. Mechanical characterization of

- bulk Sylgard 184 for microfluidics and microengineering. J Micromech Microeng 2014;24:035017.
- [19] Kida N, Ito M, Yatsuyanagi F, Kaido H. Studies on the structure and formation mechanism of carbon gel in the carbon black filled polyisoprene rubber composite. J Appl Polym Sci 1996;61:1345–50.
- [20] Berriot J, Martin F, Montes H, Monnerie L, Sotta P. Reinforcement of model filled elastomers: characterization of the crosslinking density at the filler-elastomer interface by ¹H NMR measurements. Polymer 2003;44:1437–47.
- [21] Sargsyan A, Tonoyan A, Davtyan S, Schick C. The amount of immobilized polymer in PMMA SiO₂ nanocomposites determined from calorimetric data. Eur Polym J 2007;43:3113–27.
- [22] Valentin JL, Mora-Barrantes I, Carretero-Gonzalez J, Lopez-Manchado MA, Sotta P, Long DR, Saalwächter K. Uncertainties in the determination of cross-link density by equilibrium swelling experiments in natural rubber. Macromolecules 2008:41:4717–29.
- [23] Kropka JM, Sakai VG, Green PF. Local polymer dynamics in polymer-C60 mixtures. Nano Lett 2008;8:1061–5.
- [24] Valentin JL, Mora-Barrantes I, Carretero-Gonzalez J, Lopez-Manchado MA, Sotta P, Long DR, Saalwächter K. Novel experimental approach to evaluate filler-elastomer interactions. Macromolecules 2010;43:334–46.
- [25] Mujtaba A, Keller M, Ilisch S, Radusch H-J, Thurn-Albrecht T, Saalwächter K, Beiner M. Mechanical properties and cross-link density of styrene-butadiene model composites containing fillers with bimodal particle size distribution. Macromolecules 2012:45:6504-15.
- [26] Sarkawi SS, Dierkes WK, Noordermeer JWM. Elucidation of filler-to-filler and filler-to-rubber interactions in silica-reinforced natural rubber by TEM network visualization. Eur Polym J 2014;54:118–27.
- [27] Song Y, Zheng Q. Concepts and conflicts in nanoparticles reinforcement to polymers beyond hydrodynamics. Prog Mater Sci 2016;84:1–58.
- [28] Derjaguin BV, Muller VM, Toporov YP. Effect of contact deformations on the adhesion of particles. J Colloid Interface Sci 1975;53:314–26.
- [29] Song J, Tranchida D, Vancso GJ. Contact mechanics of UV/Ozone-treated PDMS by AFM and JKR testing: mechanical performance from nano- to micrometer length scales. Macromolecules 2008;41:6757–62.
- [30] Lopez-Pamies O, Goudarzi T, Nakamura T. The nonlinear elastic response of suspensions of rigid inclusions in rubber: I — An exact result for dilute suspensions. J Mech Phys Solid 2013;61:1–18.
- [31] Lopez-Pamies O, Goudarzi T, Danas D. The nonlinear elastic response of suspensions of rigid inclusions in rubber: II A simple explicit approximation for finite-concentration suspensions. J Mech Phys Solid 2013;61:19–37.
- [32] Lopez-Pamies O. Elastic dielectric composites: Theory and application to particlefilled ideal dielectrics. J Mech Phys Solid 2014;64:61–82.
- [33] Lopez-Pamies O. A new I₁-based hyperelastic model for rubber elastic materials. Compt Rendus Mec 2010:338:3–11.
- [34] Nunes LCS, Moreira DC. Simple shear under large deformation: experimental and theoretical analyses. Eur J Mech Solid 2010;42:315–22.
- [35] Lewis TJ. Interfaces are the dominant feature of dielectrics at the nanometric level. IEEE Trans Dielectr Electr Insul 2004;11:739–53.
- [36] Nelson JK, editor. Dielectric polymer nanocomposites. New York: Springer; 2010.
- [37] Lopez-Pamies O, Goudarzi T, Meddeb AB, Ounaies Z. Extreme enhancement and reduction of the dielectric response of polymer nanoparticulate composites via interphasial charges. Appl Phys Lett 2014;104:242904.
- [38] Lefèvre V, Lopez-Pamies O. Homogenization of elastic dielectric composites with rapidly oscillating passive and active source terms. SIAM J Appl Math 2017;77:1962–88.
- [39] Lefèvre V, Danas K, Lopez-Pamies O. A general result for the magnetoelastic response of isotropic suspensions of iron and ferrofluid particles in rubber, with applications to spherical and cylindrical specimens. J Mech Phys Solid 2017;107:343–64.